THE PROTEIN SOCIETY | WILEY

FULL-LENGTH PAPER

A competition smFRET assay to study ligand-induced conformational changes of the dengue virus protease

Hannah Maus[1] | **Gerald Hinze**[2] | **Stefan Josef Hammerschmidt**[1] | **Thomas Basché**[2] | **Tanja Schirmeister**[1]

[1]Institute for Pharmaceutical and Biomedical Sciences, Johannes Gutenberg-University, Mainz, Germany

[2]Department of Chemistry, Johannes Gutenberg-University, Mainz, Germany

Correspondence
Thomas Basché, Department of Chemistry, Johannes Gutenberg-University, Mainz, Germany.
Email: thomas.basche@uni-mainz.de

Tanja Schirmeister, Institute for Pharmaceutical and Biomedical Sciences, Johannes Gutenberg-University, Mainz, Germany.
Email: schirmei@uni-mainz.de

Review Editor: Aitziber L. Cortajarena

Abstract

Ligand binding to proteins often is accompanied by conformational transitions. Here, we describe a competition assay based on single molecule Förster resonance energy transfer (smFRET) to investigate the ligand-induced conformational changes of the dengue virus (DENV) NS2B-NS3 protease, which can adopt at least two different conformations. First, a competitive ligand was used to stabilize the closed conformation of the protease. Subsequent addition of the allosteric inhibitor reduced the fraction of the closed conformation and simultaneously increased the fraction of the open conformation, demonstrating that the allosteric inhibitor stabilizes the open conformation. In addition, the proportions of open and closed conformations at different concentrations of the allosteric inhibitor were used to determine its binding affinity to the protease. The K_D value observed is in accordance with the IC_{50} determined in the fluorometric assay. Our novel approach appears to be a valuable tool to study conformational transitions of other proteases and enzymes.

KEYWORDS
allosteric inhibition, competition assay, conformational change, flavivirus, NS2B-NS3 protease, smFRET

1 | INTRODUCTION

Understanding the operating mechanism of proteins is essential for the development of new effective inhibitors.

In many cases, ligand binding leads to changes of the secondary and tertiary structure, as well as the dynamics of the proteins.[1] Various approaches already exist for tracking of ligand-induced conformational changes. For several proteins, known to undergo a conformational transition upon ligand binding (e.g., EF-hand proteins, maltose-binding protein, integrin I domains), residues have been mutated to clearly favor one of the states over the other, enabling investigation of their respective properties.[2–8]

Abbreviations: CI, combination index; DENV, dengue virus; FRET, Förster Resonance energy transfer; E_{ET}^*, FRET efficiency; I_a, allosteric inhibitor; IC_{50}, inhibitor concentration at half maximal inhibition; K_D, binding affinity; K_i^{app}, apparent K_i; NS, non-structural; NS3pro, NS3 protease; R_0, Förster Radius; smFRET, single molecule FRET; τ, fluorescence lifetime.

However, additional tools are needed to obtain information about the relationship of protein sequence, dynamics, and function. NMR or single molecule Förster resonance energy transfer (smFRET) have proven to be suitable tools for studying population distributions of conformational substrates in solution.[9–16]

The dengue virus (DENV) NS2B-NS3 protease is essential for viral replication of the virus.[17] Besides host proteases, it is responsible for the cleavage of the viral precursor polyprotein, which is translated from the single-stranded RNA genome.[17] The protease thus represents an interesting drug target for countering DENV infections. The NS3 protease (NS3$_{pro}$) is a trypsin-like serine protease with the catalytic triad His51, Asp75, and Ser135.[18] Correct folding and catalytic activity of NS3$_{pro}$ strongly depends on the presence of the cofactor NS2B.[19,20] The latter can adopt at least two different conformations, which mainly differ in their relative position compared to the active center of NS3$_{pro}$. The two conformations are designated as "open" and "closed."[21–25] As already deduced from crystal structures, the binding of ligands to the active site leads to the stabilization of the closed conformation in which NS2B wraps around the NS3$_{pro}$ domain. Thus, the closed conformation is considered the active conformation.[21] In the open conformation, however, NS2B does not contribute to substrate recognition and is rather loosely bound to NS3$_{pro}$.[22,23,26] Although crystal structures provide important and fundamental information about proteins, they only represent energy minimized snapshots and, thus, do only provide very limited information about the state and dynamics of proteins in solution.

By using NMR spectroscopy, the conformational dynamics of the DENV protease in solution was previously investigated.[12,27] Hereby, at least two species were detected, and interpreted as different conformations. The ratio of the two species could be shifted by adding a competitive inhibitor or by changing the pH value of the buffer.[12] The use of a split-luciferase assay also enabled to observe conformational dynamics in solution. In this experiment, the addition of competitive inhibitors indicated the formation of the closed conformation, which was prevented by the addition of allosteric inhibitors.[24] However, the earlier studies have limitations in their information content. In the case of the NMR studies, it was reported that the competitive inhibitors did stabilize the closed conformation and in the case of the split luciferase assay, that the allosteric inhibitors did not stabilize this conformation. Hence, none of these studies unraveled which conformation is induced by allosteric inhibitors so that their effects on the DENV protease are not yet sufficiently understood. However, to design potential inhibitors, understanding the addressed protein is essential. This knowledge includes kinetics of the protein as well as the protein's mode of operation. For rational drug design in particular, the binding pocket with which a ligand interacts must be known. Accordingly, it is of great importance to know the conformation that is stabilized by the ligand. Since there is no direct proof that allosteric inhibitors do stabilize the open conformation, the impact of an allosteric inhibitor on the conformation of the protease will be in the focus of the present work. smFRET enables to observe conformational subpopulations, conformational transitions and temporal fluctuations that typically remain elusive in ensemble measurements.[28,29] Using this method, it was already shown that the DENV protease in solution is in an equilibrium between two conformations and that the presence of a competitive inhibitor stabilizes the closed conformation.[16]

Here, we provide evidence that the allosteric inhibitor stabilizes the open conformation of the protease by applying a competition smFRET assay. Our approach is based on the initial shift of the equilibrium between open and closed conformation toward the closed conformation by the addition of a competitive inhibitor I_c (Figure 1),[30] following work by Götz et al.[16] The subsequent addition of an allosteric inhibitor I_a (Figure 1)[31] leads to a competition between the two inhibitors in a way that the
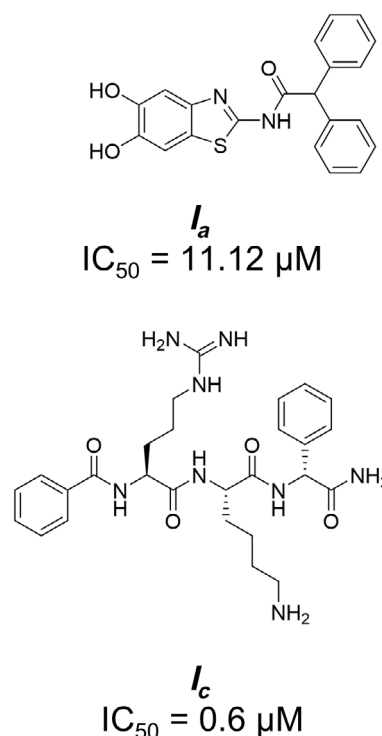

FIGURE 1 Structures and IC50 values of the allosteric (I_a)[31] and the competitive (I$_C$)[30] inhibitor

conformational equilibrium is shifted to the open conformation with increasing concentration of the inhibitor I_a. Under the experimental conditions, the concentration of I_c remains constant. For sufficiently high concentrations of I_a, an almost complete shift of the equilibrium towards the open conformation was achieved. Moreover, by evaluating the ratio between open and closed conformations the binding affinity of the allosteric inhibitor was determined. To the best of our knowledge, an assay as presented here has not been described in the literature before.

2 | RESULTS AND DISCUSSION

2.1 | FRET pair labeled DENV protease mutants

Since the DENV protease does not contain native cysteines, single cysteines can be introduced by site-directed mutagenesis and subsequently specifically labeled with dye molecules. As previously described,[16] the positions of the cysteines were chosen in a way that one of them is localized in the NS3pro domain (S158C) and the other one in the NS2B cofactor (S79C) (Figure 2).

The positions were selected to show significant distance changes between the mutated positions upon conformational changes.[16] Distances of the dyes ATTO 488 and ATTO 643 in the open and closed conformation were calculated using a toolkit from Seidel's laboratory.[32] Since the structure of ATTO 643 was not accessible, the structure of the related ATTO 647N was used for this calculation.[33] In each case, an ellipsoid was defined around the chromophore whose radii were determined using the python algorithm mol-ellipsize.[34] For this purpose, the lowest-energy conformers of the dyes including the linker were calculated using RDKit ETKDG (universal force field)[35] and the centers of mass of the chromophores as well as the linker lengths were computed using the custom PyMol center of mass plugin.[36] The resulting radii and linker lengths (Figure S1) were then used to estimate the mean distances between the dyes (Table 1). According to the data in Table 1, the distance in the open conformation is close to the Förster radius $R_0 = 5.2$ nm of the dye pair calculated by the same program.

Since the two cysteines were statistically labeled with ATTO 488 and ATTO 643, both equipped with maleimide linkers, a mixture of donor-only, acceptor-only, and donor-acceptor labeled proteases was obtained. However, in the smFRET experiments, exclusively molecules carrying one donor and one acceptor dye are informative and were considered for data analysis of fluorescence measurements. The activity of the labeled proteases was confirmed in a fluorometric assay by using a fluorogenic peptide substrate (Boc-GRR-AMC). The increase in fluorescence intensity as a function of time was used as a measure of activity. The proteolytic cleavage of the substrate releases AMC, whose fluorescence was measured at 460 nm. The unchanged turnover rate of the fluorogenic substrate of the S79C-S158C mutant and the dye-labeled mutant compared to the wild type shows that neither the mutations nor the dye labeling had a negative effect on the activity of the enzyme (Figure S3).

To determine the dye-to-protein ratio, the absorbance was measured at 280 nm (protein), 500 nm (ATTO 488), and 630 nm (ATTO 643). Degrees of labeling were determined to be 59% for ATTO 488 and 74% for ATTO 643. Binding of the dyes to the protease was examined using an SDS-PAGE gel. The scan at excitation wavelengths of 500 nm (iii, Figure 3b) and 630 nm (iv, Figure 3b), respectively, gave rise to a band at about 35 kDa in each
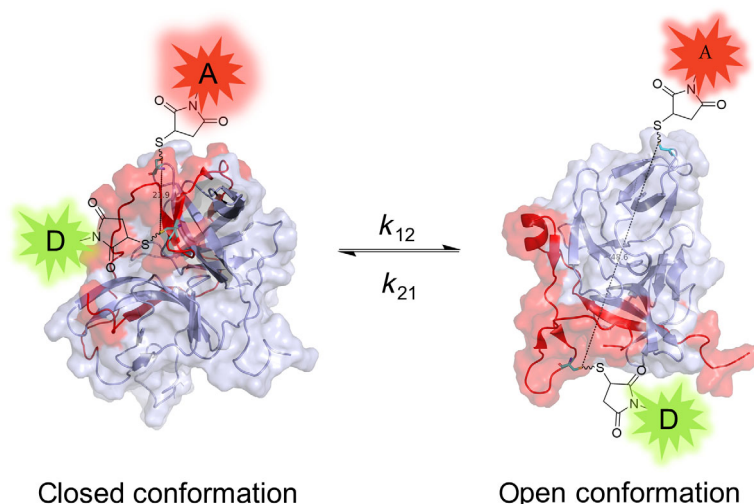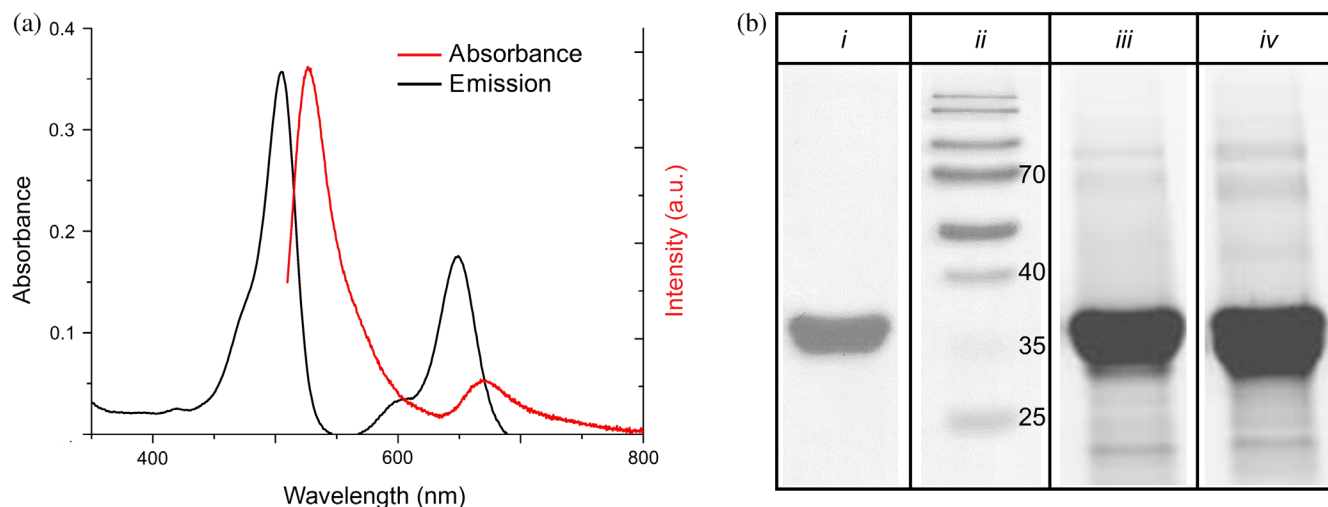

FIGURE 2 FRET pair labeled S79C-S158C double mutant of the DENV protease in the open and closed conformation. In the closed conformation (left), the distance between the dye labels is smaller than in the open conformation (right). DENV, dengue virus; FRET, Förster resonance energy transfer

Closed conformation   Open conformation

T A B L E 1 Mean distances of the dye pairs in the NS2B-NS3 protease in the open and closed conformation calculated by the toolkit from Seidel's laboratory[32]

	Dye label NS2B	Dye label NS3$_{pro}$	Mean distance (nm)
Open (2FOM)	ATTO 488-Maleimide	ATTO 647N-Maleimide	5.9 ± 0.5
	ATTO 647N-Maleimide	ATTO 488-Maleimide	5.8 ± 0.5
Closed (2M9P)	ATTO 488-Maleimide	ATTO 647 N-Maleimide	2.9 ± 0.7
	ATTO 647N-Maleimide	ATTO 488-Maleimide	3.0 ± 0.6

F I G U R E 3 Ensemble spectra of the S79C-S158C DENV protease double mutant labeled with the ATTO 488/ATTO 643 FRET pair in buffer containing 10 vol% of DMSO and SDS PAGE gel of the labeled protease. (a) Absorption (black) and emission (red) spectra. The latter was measured at 500 nm excitation. (b) SDS-PAGE gel of ATTO 488/ATTO 643 FRET pair labeled DENV protease. (i) Coomassie stain, (ii) marker PageRuler™ Prestained protein ladder (in kDa), (iii) laser scan with excitation at 500 nm, (iv) laser scan with excitation at 630 nm. DENV, dengue virus

case, in accordance with the protein band visualized by coomassie staining (i, Figure 3b).

Absorption and fluorescence emission spectra of the ATTO 488/ATTO 643 FRET pair labeled S79C-S158C double mutant of the DENV protease recorded in buffer (50 mM TRIS–HCl pH 9.0, 1 mM CHAPS) with 10 vol% of DMSO are shown in Figure 3a. These conditions correspond to the conditions during smFRET measurements. The buffer was adapted to the assay conditions known from the literature,[31,37] including the DMSO added to ensure the solubility of the inhibitors. Under these conditions, the quantum yields of the dyes were also determined. High quantum yields of over 80% were obtained for both dyes, showing that the experimental conditions are favorable for both the protease and the dyes.

2.2 | S79C-S158C DENV NS2B-NS3 ATTO 488/ATTO 643 ± allosteric inhibitor I_a

In smFRET experiments in solution, individual photon bursts from dye labeled proteins diffusing through the excitation volume are monitored and analyzed to identify subpopulations of a typically heterogeneous ensemble.[38,39] Ideally, all intrinsic parameters of the fluorophore are detected simultaneously for each burst.[40,41] These parameters include the fluorescence wavelength,[42] intensity and lifetime.[39] Here, the emission wavelengths of individual bursts were not determined, however, a separation in terms of donor or acceptor fluorescence, respectively, was implemented.

To increase the stability of the allosteric inhibitor over the duration of the measurements, 1 mM TCEP was added to the buffer, in deviation from the previously used assay conditions.[31] The double mutant labeled with ATTO 488 and ATTO 643 was excited at 502 nm and the stream of emitted photons was recorded with and without the allosteric inhibitor at a concentration of 200 μM of the latter.[31]

For further evaluation, fluorescence intensity time traces with a binning time of 1 ms were calculated from the fluorescence bursts, considering only bursts which showed a total of at least 20 counts on both APDs. Sections of the intensity time traces of ATTO 488/ATTO

643 labeled S79C-S158C DENV protease with and without inhibitor are presented in Figure 4.

Auto- and cross-correlations were then calculated from the collected data. The cross-correlation G_{AD} after addition of the allosteric inhibitor (I_a) drops faster to zero than G_{AD} without I_a (Figure 5). This observation indicates the stabilization of one conformation by addition of I_a. It is noteworthy that the cross-correlation G_{AD} consists of a diffusion term and in case of fluctuating FRET dynamics an additional rise term, describing the exchange rates between different FRET states. Thus,
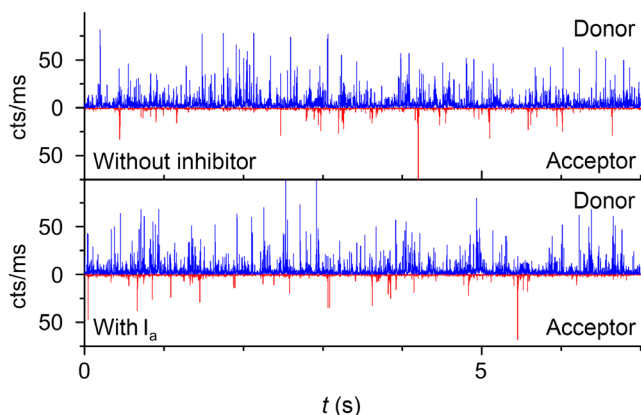
FIGURE 4   Section of the fluorescence intensity time trace of ATTO 488/ATTO 643 FRET pair labeled DENV protease with and without 200 μM of the allosteric inhibitor. The sample was excited with excitation pulses at 502 nm. The binning time was 1 ms. the donor channel is shown in blue, the acceptor channel is shown in red. DENV, dengue virus
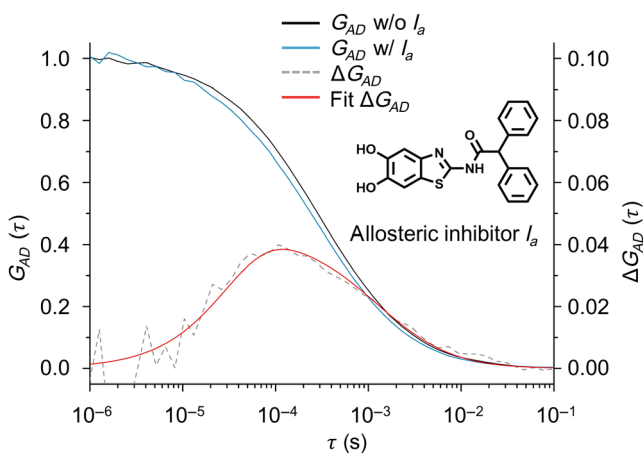

FIGURE 5   Cross-correlations (GAD) of the ATTO 488 and ATTO 643 labeled DENV protease S79C-S158C double mutant before (black) and after addition (blue) of 200 μM of the allosteric inhibitor (I_a).[31] The difference function ΔGAD of the cross-correlations is shown as a dashed line, the corresponding fit in red. DENV, dengue virus

fluctuating FRET dynamics effectively delay the decay of the cross-correlation G_{AD} compared to pure diffusion. Accordingly, the observation of a faster decay indicates less FRET dynamics or the stabilization of one conformation by addition of I_a. Neither triplet kinetics[43] nor quantum yields depending on I_a should affect the normalized cross-correlation.

As seen in Figure 5, the effect is rather moderate, and no conclusion can be drawn from the cross-correlation regarding which conformation is stabilized. Under the assumption that I_a stabilizes a conformation of the protease for at least the period of observation, a difference function (ΔG_{AD}) can be calculated from the correlation functions according to Torres et al.[44] The exchange correlation time ($(k_{12} + k_{21})^{-1}$) was estimated to be ~32 μs from the corresponding difference function (Appendix S1).

A burst analysis was performed, resulting in 2D histograms (Figure 6). Before (Figure 6a) and after addition (Figure 6b) of I_a, distinct point clouds can be seen in the 2D histograms. However, no shift of the E^*_{ET} frequency distributions was observed.

While from both, donor and acceptor, 2D histograms are available, point clouds at $E^*_{ET} > 0.5$ are better visible in the acceptor 2D histograms. Moreover, with increasing number of acceptor photons within a burst, the statistical significance of the calculated fluorescence lifetimes
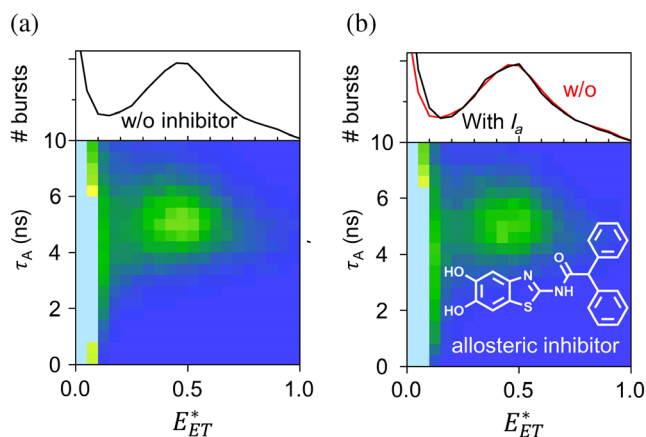
FIGURE 6   Plot of the normalized occurrences of the individual bursts (individual molecules) within the intensity time trace of the ATTO 488/ATTO 643 FRET pair labeled DENV protease in a 2D histogram, separated according to acceptor lifetime τ_A and FRET efficiency E^*_{ET}. (a) without allosteric inhibitor. (b) Black: With allosteric inhibitor ($I_a = 200$ μM), red: Without allosteric inhibitor. For an easier visual comparison of the FRET populations before and after addition of the inhibitor, the respective maxima were normalized to one. The respective normalized 1D histograms of FRET efficiencies are shown as a projection on the top of the 2D histograms. DENV, dengue virus; FRET, Förster resonance energy transfer

increases. Finally, counts in the acceptor channel mainly originate from FRET pair labeled protease, while in the donor channel donor–donor labeled protease and Raman scattering contribute as well. Therefore, we omit the data from the donor channel and will focus only on the acceptor 2D histograms.

In the 2D histogram, the acceptor lifetime τ_A, which was obtained as the mean delay time of the fluorescence of the acceptor dye without taking the instrumental response function (IRF) into account, is plotted against E_{ET}^* from the intensity ratios per burst. A change of the energy transfer efficiency leads to a shift of the point cloud, respectively the formation of an additional point cloud, which differs from the first one in its position of E_{ET}^* as well as of τ_A. To make even small changes visible, it is useful to examine the 2D diagrams in addition to the 1D histograms of the E_{ET}^* frequency distributions.

As seen in Figure 6, the point cloud is already located at intermediate FRET efficiencies before the addition of the allosteric inhibitor. In line with the observations of Zhu et al., who reported the prevalence of the open conformation of the protease at high pH values,[12] we conclude that the intermediate transfer efficiency of $E_{ET}^* \sim 0.5$ represents the open conformation. Accordingly, at this point the absence of a shift to higher FRET efficiencies in the presence of the allosteric inhibitor only indicates that the inhibitor does not stabilize the closed conformation. To reveal a potential shift of the conformational equilibrium of the protease in solution towards the open conformation by the addition of an allosteric inhibitor, the former approach had to be extended and a competition assay was designed.

2.3 | Competition assay

The conformation of the protease in solution depends on the pH value in the manner that the equilibrium of the two conformations is on the side of the open conformation at high pH values.[12] As a consequence, in our experiments performed at pH 9.0, only stimuli that lead to the stabilization of the closed conformation can be directly investigated. Note that the experimental conditions were adapted to the conditions during the fluorometric assay (50 mM Tris, 1 mM CHAPS, pH 9.0).[31,37]

It is assumed that the addition of allosteric inhibitors leads to the stabilization of the open conformation.[24] Therefore, to investigate the influence of an allosteric inhibitor on the conformation of the protease, a competition assay was designed.

To implement this approach, the stabilization of the closed conformation by a competitive inhibitor[30] was exploited to obtain a significant fraction of proteases in

the closed conformation prior to addition of an allosteric inhibitor. Only then a shift of the equilibrium towards the open conformation could be observed. For this purpose, we first investigated whether different concentrations of the competitive inhibitor resulted in varying populations of the closed conformation. Indeed, as seen in Figure 7 the E_{ET}^* frequency distributions support the growth of the closed conformation with increasing concentration of the competitive inhibitor.

For the competition assay, a concentration of 2 μM of the competitive inhibitor was used. At this concentration, two distinct populations of protease can be seen in the frequency distribution of E_{ET}^* (Figure 7). Experiments were performed with different concentrations of the allosteric inhibitor (0.1–167 μM) while keeping the concentration of the competitive inhibitor constant. The collected fluorescence data were then subjected to burst analysis.

The E_{ET}^* frequency distributions show two distinct populations (Figure 8a,c) that can be interpreted as the open ($E_{ET}^* \sim 0.4 - 0.6$) and closed ($E_{ET}^* \sim 0.7 - 1.0$) conformation. As the concentration of I_a did increase, the fraction of the population of the closed conformation was reduced while the fraction of the open conformation was increased. This is a clear indication that the allosteric inhibitor stabilizes the open conformation of the protease. To determine the binding affinity, the ratio between open and closed conformations was determined using two different analysis methods. First, this ratio was derived from the cumulative integrals of the E_{ET}^* frequency distributions (Figure 8b). After normalization in the range of $E_{ET}^* \sim 0.4 - 0.6$, the cumulative integral P_i
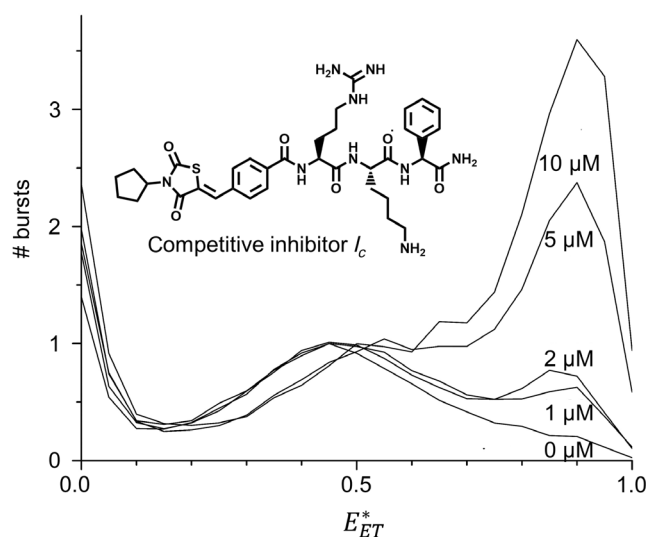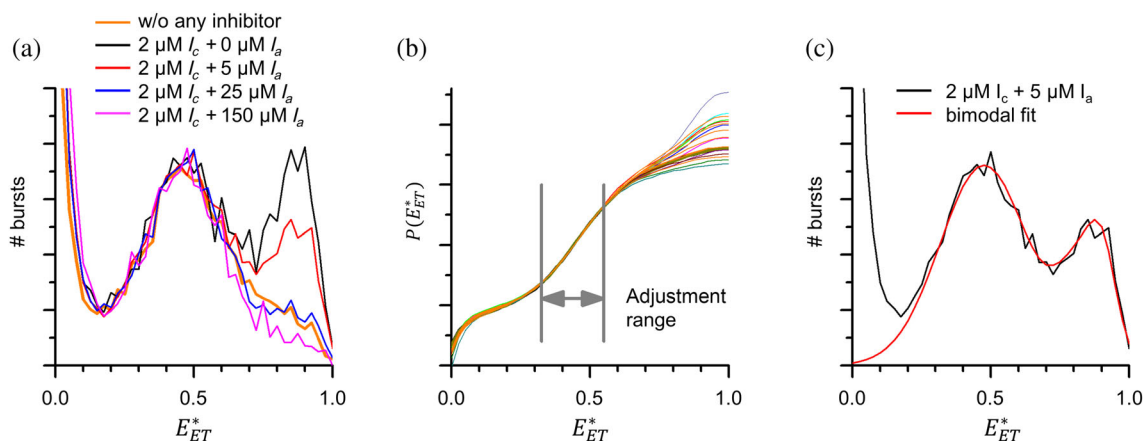

FIGURE 7 E_{ET}^* frequency distributions of ATTO 488/ATTO 643 FRET pair labeled DENV protease with different concentrations of the competitive inhibitor.[30] DENV, dengue virus; FRET, Förster resonance energy transfer
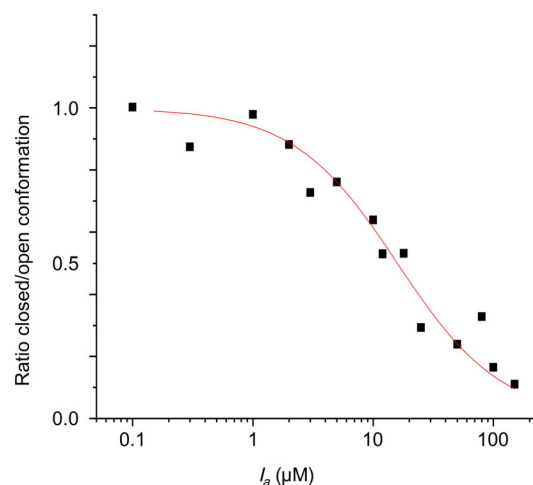
FIGURE 8 E_{ET}^* frequency distributions of the competition smFRET assay. (a) E_{ET}^* frequency distributions of ATTO 488/ATTO 643 FRET pair labeled DENV protease with different concentrations of the allosteric inhibitor (0–150 µM) in the presence of 2 µM of the competitive inhibitor. (b) Cumulative integrals of E_{ET}^* frequency distributions of ATTO 488/ATTO 643 FRET pair labeled DENV protease with different concentrations of the allosteric inhibitor (0–167 µM) in the presence of 2 µM of the competitive inhibitor normalized in the range of $E_{ET}^* \sim 0.4$–0.6. (c) Exemplary bimodal fit for the E_{ET}^* frequency distribution of ATTO 488/ATTO 643 FRET pair labeled DENV protease with 2 µM of the competitive inhibitor and 5 µM of the allosteric inhibitor. DENV, dengue virus; smFRET, single molecule Förster resonance energy transfer

was determined at $E_{ET}^* = 1.0$ and plotted against the concentration of the inhibitor resulting in a sigmoidal affinity curve (Figure 9). The binding affinity $K_D = 15.9 \pm 2.5$ µM of the inhibitor was obtained from the inflection point of the sigmoidal curve. For the second analysis method, the E_{ET}^* frequency distributions were simply approximated by a bimodal fit composed of three Gaussians which turned out to satisfactorily reproduce the data. (Figure 8c) The ratio between open and closed conformation was then determined as the ratio of the corresponding amplitudes. The amplitude ratios were again plotted against the inhibitor concentration, yielding a K_D of 11.7 ± 2.2 µM (Figure S7).

The binding affinities obtained with these two methods are very similar and both are within the same range as the IC$_{50}$ determined in the fluorometric assay under the same buffer conditions (IC$_{50}$ = 12.8 ± 0.8 µM, Figure S4) and the apparent K_i (K_i^{app}) obtained from the Dixon plot (K_i^{app} = 14.7 ± 3.7 µM, Figure S8).

2.4 | Inhibitor combination studies

Using the Chou-Talalay method, the impact of a combination of inhibitors was investigated.[45] IC$_{50}$ values of the competitive and allosteric inhibitor were determined separately and in combination using a fluorometric assay (Figures S4−S6). Both compounds were subjected to assays at 7 concentrations at least, starting from the minimum dose required for the enzyme inhibition to that necessary to fully suppress protease activity. IC$_{50}$ values have been obtained from dose response curves (Figures S4−S6). According to

FIGURE 9 Binding affinity curve determined from the competitive smFRET assay based on the evaluation of the cumulative integrals of the E_{ET}^* frequency distributions. The sigmoidal fit provides a binding affinity of the allosteric inhibitor of $K_D = 15.9 \pm 2.5$ µM. smFRET, single molecule Förster resonance energy transfer

their IC$_{50}$ values, I_c and I_a were used in a 1:2 ratio in the combination study. The combination index (CI) calculated using the formula for mutually non-exclusive inhibitors reads:

$$CI = \left[\frac{(D)_a}{(D_i)_a}\right] + \left[\frac{(D)_c}{(D_i)_c}\right] + \frac{[(D)_a(D)_c]}{[(D_i)_a(D_i)_c]}$$

where $(D_i)_a$ and $(D_i)_c$ represent the concentrations of I_a and I_c alone, that are necessary to produce i% of protease

TABLE 2 CI for an inhibition of i% calculated with the Chou-Talalay method for mutually non-exclusive inhibitors

| i	99%	90%	80%	70%	60%
CI	1.74	1.73	1.67	1.66	1.66
i	50%	40%	30%	20%	10%
CI	1.67	1.70	1.74	1.81	1.96

Abbreviation: CI, combination index.

inhibition, while $(D)_a$ and $(D)_c$ are the concentrations of both compounds able to produce i% of protease inhibition when they are used in combination. From the value of CI, we can infer how the combination of inhibitors affects their inhibition. When CI <1, synergism is indicated, for CI = 1 summation is indicated and CI >1 indicates antagonism. CI values were calculated for $i = 10$, 20, 30, 40, 50, 60, 70, 80, 90, and 99% inhibition of the protease (Table 2).

The calculated CI values, which are consistently greater than 1 for inhibitions between 10 and 99%, indicate antagonism of the two inhibitors. Since we cannot be sure whether the inhibitors are mutually exclusive or non-exclusive, the CI value was also calculated for exclusive inhibitors (data not shown). Here, the last summand of the above formula is not taken into account. The corresponding CI values are also higher than 1 and thus indicate antagonism. These results support our findings in the smFRET experiments, where we observed that the two inhibitors stabilize different conformations.

2.5 | Kinetic modeling

From the experiments described above, it was concluded that the open conformation is stabilized by binding of the allosteric inhibitor and that the inhibitors show antagonistic effects. To address the impact of the bound competitive inhibitor onto the binding of the allosteric inhibitor under the experimental setup, kinetic modeling was performed. Since no statement can be made about which conformation the inhibitor binds to, two different models were considered. In the following, model 1, (model 2, see Appendix S1) which assumes that the two inhibitors bind exclusively to the conformation that they stabilize (conformational selection), will be discussed in more detail. Based on this assumption, the following equilibria, with I_c as the competitive inhibitor, I_a as the allosteric inhibitor, E_c as the closed conformation of the protease, E_o as the open conformation of the protease, E_cI_c as the complex of closed conformation and competitive inhibitor, and E_oI_a as the complex of open conformation and allosteric inhibitor, can be established:

$$E_cI_c \; \xrightleftharpoons{K_{i,c}} \; I_c \; + \; E_c$$

$$\Big\Updownarrow K_c$$
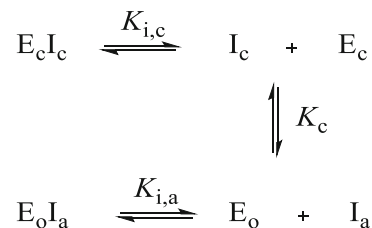
$$E_oI_a \; \xrightleftharpoons{K_{i,a}} \; E_o \; + \; I_a$$

Thus, the following equilibrium constants can be formulated:

$$K_{i,c} = \frac{[E_c][I_c]}{[E_cI_c]}, K_{i,a} = \frac{[E_o][I_a]}{[E_oI_a]}, \text{and } K_c = \frac{[E_o]}{[E_c]}.$$

Using the equilibrium constants $K_{i,c}$, $K_{i,a}$, and K_c and the initial concentrations of the ligands $[I_a^0]$ and $[I_c^0]$, the total concentration of open $[E_o^*]$ and closed $[E_c^*]$ conformations of the protease present during the measurement can be described. Since the concentration of the protease used in the experiments is significantly smaller than the equilibrium constants $K_{i,c}$ and $K_{i,a}$, the following approximations can be made:

$$[E_c^*] \cong [E_c]\left(1 + \frac{[I_c^0]}{K_{i,c}}\right) \text{ and } [E_o^*] \cong [E_o]\left(1 + \frac{[I_a^0]}{K_{i,a}}\right).$$

The relationship between the closed and the open conformation can be described by the following term

$$\frac{[E_c^*]}{[E_o^*]} = F\frac{1}{\left(1 + \frac{[I_a^0]}{K_{i,a}}\right)},$$

where $F = K_c^{-1}\left(1 + \frac{[I_c^0]}{K_{i,c}}\right)$ remains constant during the addition of the allosteric inhibitor. The resulting titration curve $T([I_a^0])$ runs independently of the concentration of the competitive inhibitor from $T(0) = F$ over $T([I_a^0] = K_{i,a}) = \frac{1}{2}F$ to $T(\infty) = 0$. As such, it qualitatively reproduces the binding affinity curve displayed in Figure 9. The second binding model (induced fit) provides similar results which are discussed in detail in Appendix S1.

Remarkably, both models showed that the binding affinity of the allosteric inhibitor is not influenced by the presence of the competitive inhibitor under the experimental conditions, although antagonism of the inhibitors was indicated in the combination study. Which of the two models is more applicable to the binding of the ligand cannot be judged from the results described herein.

The agreement between the results from the fluorometric assay and the Dixon plot on one side and the smFRET competition assay on the other side indicates that the assay is suitable for the direct determination of binding affinities. It should also be mentioned that the inhibitory activity of I_a in the fluorometric assay is determined in the presence of a substrate, which is believed to stabilize the closed conformation.

3 | CONCLUSIONS

The existence of at least two different conformations of the DENV NS2B-NS3 protease, designated open and closed, has been reported by various groups. While the impact of competitive inhibitors on the protease has already been sufficiently investigated, the effect of allosteric inhibitors remains elusive. Various approaches showed that competitive inhibitors stabilize the closed conformation of the DENV protease. In contrast, the impact of allosteric inhibitors on the conformation of the protease has been inferred exclusively from the absence of signals, which was interpreted as stabilization of the open conformation.

To investigate the effect of an allosteric inhibitor on the conformation of DENV protease, we statistically labeled a double mutant (S79C-S158C) of the protease with ATTO 488 and ATTO 643 and then performed smFRET experiments. The positions of the point mutations were chosen in such a way that their distance changes significantly with the conformation. Analysis of the fluorescence cross-correlation function of the labeled double mutant in the absence and presence of the allosteric inhibitor indicated stabilization of one conformation, but it could not be decided which of the two conformations was stabilized. Since, under our experimental conditions, the protease is mostly present in the open conformation, only stabilizations of the closed conformation could be visualized by smFRET in the presence of a competitive inhibitor. The absence of a shift to higher FRET efficiencies after addition of an allosteric inhibitor thus only indicated that the closed conformation is not stabilized.

To directly visualize a shift to the open conformation induced by an allosteric inhibitor, a competition assay was designed. This assay is based on an initial shift of the conformational equilibrium toward the closed conformation by a competitive inhibitor. This shift was noticed in the E_{ET}^* frequency distributions by the appearance of a second peak ($E_{ET} \sim 0.6 - 1.0$), clearly separated from the first peak ($E_{ET} \sim 0.4 - 0.6$) originating from the open conformation. In the presence of a constant concentration of the competitive inhibitor, a titration with an allosteric inhibitor was then performed. It was found that with increasing concentration of the allosteric inhibitor, the fraction of the open conformation of the protease in solution increased, while the fraction of the closed conformation was reduced. Accordingly, we could demonstrate that the open conformation is stabilized by the allosteric inhibitor.

The relationship between open and closed conformation was accessed in two ways. First, the ratio of the peak areas of the E_{ET}^* frequency distributions was considered. For this purpose, cumulative integrals were calculated. Secondly, the areas of the two peaks were put into relation. In this case, the E_{ET}^* frequency distributions were approximated by appropriate functions. The outcomes of both methods, when plotted against the concentration of the allosteric inhibitor, allowed the determination of the binding affinity. The K_D values are in good agreement with the IC_{50} value determined by a fluorometric assay or the K_i^{app}, constant determined by a Dixon plot. The similarity of these values seems to indicate that equilibrium kinetics sufficiently describes the interplay of both inhibitors and the protease. This assumption was justified by kinetic modeling which showed that the presence of the competitive inhibitor has no effect on the binding affinity of the allosteric inhibitor.

The competition smFRET assay developed in this work appears as a promising tool to study ligand-protein interactions. As such, the methodology can be transferred to other enzymes that undergo conformational changes upon binding of ligands. An obvious case would be the structurally similar NS2B-NS3 protease of the Zika virus. Moreover, transfer to unrelated proteins is also conceivable.

4 | MATERIAL AND METHODS

4.1 | Protein constructs and cloning

Protein constructs were used and cloning was conducted as described by Millies et al.[37] In short, site directed mutagenesis was performed using the Kapa HiFi PCR kit (KapaBiosystems Inc., Woburn, MA) to generate the S79C and S158C mutations in a pET15b vector harboring the DENV $NS2B_{cf}$-$NS3_{pro}$ gene (GenBank ID: AY037116.1). A detailed description of protein constructs and cloning can be found in Appendix S1.

4.2 | Protein expression and purification

Protein expression and purification were performed as described by Millies et al.[37] Briefly, competent *Escherichia coli* BL21 Gold (DE3) cells (Agilent Technologies,

Santa Clara, CA) were grown in LB medium and expressed protein after induction with IPTG for 16 hr at 20°C. After harvesting and lysis of the cell pellets the resulting supernatant was subjected to an immobilized metal affinity chromatography (IMAC) on a HisTrap HP 5 ml column (GE Healthcare, Chicago, IL) and eluted in a linear gradient of buffer containing raising imidazole concentrations. Eluted fractions were further purified by size exclusion chromatography (SEC). A detailed description of protein expression and purification can be found in Appendix S1.

4.3 | Fluorescence labeling of the DENV-Protease double mutant S79C-S158C

The fluorescence labeling was performed analogously to Götz et al. using ATTO 643 instead of ATTO 647N.[16] In brief, a buffer containing TCEP was used to ensure free thiol groups within the cysteine double mutants. After an incubation time of 30 min at 4°C, TCEP was removed by rebuffering using spin concentrators. To the rebuffered protein solution were added a 2.1-fold excess of ATTO 488 and a 2.6-fold excess of ATTO 643, both dissolved in DMF. Dye labeling occurred during a 2 hr incubation time at room temperature. Labeled protease was then dialyzed and purified by SEC. For more details in Fluorescent Labeling, see Appendix S1.

4.4 | smFRET experiments

The smFRET experiments were performed analogously to the literature.[16] They were conducted in self-constructed sample cells made of a poly(ethylene glycol) coated glass coverslip and a glued-on plastic cylinder. Sample cells were loaded with 150 µl of FRET pair labeled double mutant of the protease ($c \sim 100$ pM) in buffer containing 10 vol% DMSO. Fluorescence photons were collected with a custom-built confocal microscope over a period of 1800 s. Measurements with inhibitor were performed after those without inhibitor, while the concentration of the protease and buffer conditions were kept constant. Excitation of the fluorophores was performed with a spectrally filtered output from a pulsed white light fiber laser (10 MHz, SC OEM, YSL Photonics, China). Excitation pulses were centered around 502 nm by using an acousto-optical tunable filter (AOTF-VIS-DR, Fianium, UK). Excitation and emission were separated by a dichroic mirror (ZT491 rdcxrxt-UF1, CHROMA, Bellows Falls, VT). Emitted fluorescence light was spectrally separated by a dichroic mirror (ZT640-rdc-UF1, CHROMA, Bellows Falls, VT) into red light and light of

higher energy. Both beams were then focused onto two APDs (acceptor channel A: SPCM-AQRH-15, PerkinElmer, Waltham, MA; donor channel D: PDM 50ct, MPD, Italy). The absolute and relative arrival times (relative to excitation pulse) of the individual photons were detected by a HydraHarp 400 module (PicoQuant, Germany) which was connected to the two detector APDs. Further details on smFRET experiments can be found in Appendix S1.

4.5 | Analysis of smFRET data

The data were analyzed as described by Götz et al.[16] Cross-correlation functions $G_{AD}(\tau)$ (FCS-FRET) were calculated from the arrival times of the individual photons. Individual bursts extracted from the fluorescence intensity time traces (bin time = 1 ms) were analyzed. Bursts with at least 20 counts on both APDs were considered for further evaluation. Average arrival times τ_A of the acceptor photons relative to the excitation pulse (without taking the IRF into account) were calculated for each individual burst. The IRF was recorded at the beginning of each measurement day. The full width at half-maximum height (FWHM) was about 770 ps. The FRET efficiency E_{ET}^* was calculated for each burst:

$$E_{ET}^* = \frac{\text{counts}(A)}{\text{counts}(A) + \text{counts}(D)}.$$

The individual bursts were sorted with respect to their E_{ET}^* values and presented in frequency distributions. Details on the analysis of smFRET data can be found in Appendix S1.

4.6 | Analysis of competition assay

1. The cumulative integrals of the distributions of the FRET efficiencies $P(E_{ET})$ were calculated and normalized to each other in the range of the mean FRET efficiency ($E_{ET} \sim 0.4 - 0.6$). For this purpose, normalization factors f_i were determined so that the maxima of $V_{i,norm}(E_{ET}) = f_i \cdot V_i(E_{ET})$ overlap.

$$P_i(E_{ET}) = \int_0^{E_{ET}} V_i(E'_{ET}) dE'_{ET}$$

For a normalization of the cumulative distributions $P_i(E_{ET})$ in the corresponding range, an adjusted intercept b_i is necessary in addition to a stretching factor m_i, which considers the different contributions at small $E_{ET} < 0.4$,

that is, $\int_{0.4}^{} V_i(E'_{ET})dE'_{ET}$. The determination of the normalization pairs (m_i, b_i) was done via linear regression. From the values $P_i(E_{ET} = 1.0)$, after subtracting an unknown offset, the proportions of the closed conformation for the individual measurements i could be determined. The offset B_{offset} was treated as a fit parameter. The $P_i(E_{ET} = 1.0, [I_a^0])$ obtained at different concentrations of the allosteric inhibitor were plotted as a function of the concentration of the allosteric inhibitor $[I_a^0]$. Titration curves were obtained by applying a global fit $P_i(E_{ET} = 1.0, [I_a^0]) = A_j \frac{1}{\left(1 + \frac{[I_a^0]}{K_{i,a}}\right)} + B_{offset}$.

The measurements for the competition assay were performed on three independent measuring days. Since each measurement differs due to the individual adjustment of the microscope and the exact protease concentrations used, a factor A_j was introduced to compensate these deviations.

2. For alternative evaluation, the E_{ET}^* frequency distributions were represented by a fit with a bimodal distribution composed of three Gaussians. For the range $E_{ET} \sim 0.4 - 0.6$ a Gaussian distribution with the parameters $E_{ET,1} = 0.47560$ und $\sigma_1 = 0.15927$ (both determined) was assumed.

$$G_1(E_{ET}) = M_1 \, exp\left(-\frac{(E_{ET} - E_{ET,1})^2}{2\sigma_1^2}\right)$$

The distribution function for the range $E_{ET} \sim 0.7 - 1.0$ was represented by a composite function with $E_{ET,2a} = 0.90448$, $\sigma_{2a} = 0.05107$, $E_{ET,2b} = 0.82242$, and $\sigma_{2b} = 0.07923$.

$$G_2(E_{ET}) = M_2 \left[0.899 \cdot exp\left(-\frac{(E_{ET} - E_{ET,2a})^2}{2\sigma_{2a}^2}\right) + exp\left(-\frac{(E_{ET} - E_{ET,2b})^2}{2\sigma_{2b}^2}\right)\right]$$

For each distribution $V_i(E_{ET})$, the amplitude ratios $M_{2,i}/M_{1,i}$ were determined and plotted as a function of the concentration of the allosteric inhibitor. This titration curve was approximated by a global fit from which the binding affinity was determined as the inflection point.

4.7 | Fluorometric enzyme assay

The fluorometric assay was performed mainly as described in the literature.[31] Briefly, 250 nM of the protease in buffer (50 mM Tris–HCl pH 9.0, 1 mM CHAPS, 1 mM TCEP) with 5 μl of the substrate in DMSO and 10 μl of the corresponding inhibitor in DMSO resulting in a total volume of 200 μl was added to a 96 well plate and the fluorescence of the released AMC was measured at 380 nm excitation and 460 nm emission. The percentage activity of the protease with the addition of the inhibitors was determined as the proportion of the slope with respect to the slope of the DMSO control. A detailed description can be found in Appendix S1.

AUTHOR CONTRIBUTIONS

Hannah Maus: Data curation (lead); validation (equal); writing – original draft (equal); writing – review and editing (equal). **Gerald Hinze:** Formal analysis (lead); software (lead); validation (equal); writing – original draft (equal); writing – review and editing (equal). **Stefan Josef Hammerschmidt:** Data curation (supporting); writing – original draft (equal); writing – review and editing (equal). **Thomas Basché:** Conceptualization (equal); funding acquisition (equal); project administration (equal); supervision (equal); writing – original draft (equal); writing – review and editing (equal). **Tanja Schirmeister:** Conceptualization (equal); funding acquisition (equal); project administration (equal); supervision (equal); writing – original draft (equal); writing – review and editing (equal).

DATA AVAILABILITY STATEMENT

Data available on request from the authors

ORCID

Hannah Maus https://orcid.org/0000-0002-3512-5626
Stefan Josef Hammerschmidt https://orcid.org/0000-0002-0769-8435
Thomas Basché https://orcid.org/0000-0003-0502-7088
Tanja Schirmeister https://orcid.org/0000-0002-4587-5076

REFERENCES

1. Mizoue LS, Chazin WJ. Engineering and design of ligand-induced conformational change in proteins. Curr Opin Struct Biol. 2002;12(4):459–63. https://doi.org/10.1016/S0959-440X(02)00348-2

2. Ababou A, Shenvi RA, Desjarlais JR. Long-range effects on calcium binding and conformational change in the N-domain of Calmodulin. Biochemistry. 2001;40(42):12719–26. https://doi.org/10.1021/bi010405b

3. Nelson MR, Thulin E, Fagan PA, Forsén S, Chazin WJ. The EF-hand domain: a globally cooperative structural unit. Protein Sci. 2009;11(2):198–205. https://doi.org/10.1110/ps.33302

4. Ababou A. Solvation energetics and conformational change in EF-hand proteins. Protein Sci. 2001;10(2):301–12. https://doi.org/10.1110/ps.33601

5. Marvin JS, Hellinga HW. Manipulation of ligand binding affinity by exploitation of conformational coupling. Nat Struct Biol. 2001;8(9):795–8. https://doi.org/10.1038/nsb0901-795

6. Benson DE, Haddy AE, Hellinga HW. Converting a maltose receptor into a nascent binuclear copper oxygenase by computational design. Biochemistry. 2002;41(9):3262–9. https://doi.org/10.1021/bi011359i

7. Shimaoka M, Shifman JM, Jing H, Takagi J, Mayo SL, Springer TA. Computational design of an integrin I domain stabilized in the open high affinity conformation. Nat Struct Biol. 2000;7(8):674–8. https://doi.org/10.1038/77978

8. Dahiyat BI, Sarisky CA, De Mayo SL. Novo protein design: towards fully automated sequence selection. J Mol Biol. 1997; 273(4):789–96. https://doi.org/10.1006/jmbi.1997.1341

9. Evenäs J, Thulin E, Malmendal A, Forsén S, Carlström G. NMR studies of the E140Q mutant of the carboxy-terminal domain of Calmodulin reveal global conformational exchange in the Ca2+-saturated state. Biochemistry. 1997;36(12):3448–57. https://doi.org/10.1021/bi9628275

10. Wand AJ. Dynamic activation of protein function: a view emerging from NMR spectroscopy. Nat Struct Biol. 2001;8(11): 926–31. https://doi.org/10.1038/nsb1101-926

11. Kauk M, Hoffmann C. Intramolecular and intermolecular FRET sensors for GPCRs—monitoring conformational changes and beyond. Trends Pharmacol Sci. 2018;39(2):123–35. https://doi.org/10.1016/j.tips.2017.10.011

12. Zhu L, Yang J, Li H, Sun H, Liu J, Wang J. Conformational change study of dengue virus NS2B-NS3 protease using 19F NMR spectroscopy. Biochem Biophys Res Commun. 2015; 461(4):677–80. https://doi.org/10.1016/j.bbrc.2015.04.090

13. Ha T, Ting AY, Liang J, Caldwell WB, Deniz AA, Chemla DS, et al. Single-molecule fluorescence spectroscopy of enzyme conformational dynamics and cleavage mechanism. Proc Natl Acad Sci U S A. 1999;96(3):893–8. https://doi.org/10.1073/pnas.96.3.893

14. Santoso Y, Joyce CM, Potapova O, le Reste L, Hohlbein J, Torella JP, et al. Conformational transitions in DNA polymerase I revealed by single-molecule FRET. Proc Natl Acad Sci U S A. 2010;107(2):715–20. https://doi.org/10.1073/pnas.0910909107

15. Ruer M, Krainer G, Gröger P, Schlierf M. ATPase and protease domain movements in the bacterial AAA+ protease FtsH are driven by thermal fluctuations. J Mol Biol. 2018;430(22):4592–602. https://doi.org/10.1016/j.jmb.2018.07.023

16. Götz C, Hinze G, Gellert A, Maus H, von Hammerstein F, Hammerschmidt SJ, et al. Conformational dynamics of the dengue virus protease revealed by fluorescence correlation and single-molecule FRET studies. J Phys Chem B. 2021;125(25): 6837–46. https://doi.org/10.1021/acs.jpcb.1c01797

17. Behnam MAM, Nitsche C, Boldescu V, Klein CD. The medicinal chemistry of dengue virus. J Med Chem. 2016;59(12):5622–49. https://doi.org/10.1021/acs.jmedchem.5b01653

18. Amberg SM, Nestorowicz A, McCourt DW, Rice CM. NS2B-3 Proteinase-Mediated Processing in the Yellow Fever Virus Structural Region: In Vitro and in Vivo Studies. J Virol. 1994; 68(6):3794–802.

19. Gupta G, Lim L, Song J. NMR and MD studies reveal that the isolated dengue NS3 protease is an intrinsically disordered chymotrypsin fold which absolutely requests NS2B for correct folding and functional dynamics. PLoS One. 2015;10(8):1–24. https://doi.org/10.1371/journal.pone.0134823

20. Yusof R, Clum S, Wetzel M, Murthy HMK, Padmanabhan R. Purified NS2B/NS3 serine protease of dengue virus type 2 exhibits cofactor NS2B dependence for cleavage of substrates with dibasic amino acids in vitro. J Biol Chem. 2000;275(14): 9963–9. https://doi.org/10.1074/jbc.275.14.9963

21. Noble CG, Seh CC, Chao AT, Shi PY. Ligand-bound structures of the dengue virus protease reveal the active conformation. J Virol. 2012;86(1):438–46. https://doi.org/10.1128/jvi.06225-11

22. Erbel P, Schiering N, Arcy AD, et al. Structural basis for the activation of flaviviral NS3 proteases from dengue and West Nile virus. Nat Struct Mol Biol. 2006;13(4):2005–6. https://doi.org/10.1038/nsmb1073

23. Nitsche C, Holloway S, Schirmeister T, Klein CD. Biochemistry and medicinal chemistry of the dengue virus protease. Chem Rev. 2014;114(22):11348–81. https://doi.org/10.1021/cr500233q

24. Brecher M, Li Z, Liu B, Zhang J, Koetzner CA, Alifarag A, et al. A conformational switch high-throughput screening assay and allosteric inhibition of the Flavivirus NS2B-NS3 protease. PLoS Pathog. 2017;13(5):e1006411. https://doi.org/10.1371/journal.ppat.1006411

25. Chen WN, Loscha KV, Nitsche C, Graham B, Otting G. The dengue virus NS2B-NS3 protease retains the closed conformation in the complex with BPTI. FEBS Lett. 2014;588(14):2206–11. https://doi.org/10.1016/j.febslet.2014.05.018

26. Phoo WW, El Sahili A, Zhang ZZ, et al. Crystal structures of full length DENV4 NS2B-NS3 reveal the dynamic interaction between NS2B and NS3. Antiviral Res. 2020;182(July):104900. https://doi.org/10.1016/j.antiviral.2020.104900

27. De La Cruz L, Nguyen THD, Ozawa K, et al. Binding of low molecular weight inhibitors promotes large conformational changes in the dengue virus Ns2b-Ns3 protease: fold analysis by pseudocontact shifts. J Am Chem Soc. 2011;133(47):19205–15. https://doi.org/10.1021/ja208435s

28. Bräuchle C, Lamb DC, Michaelis J. Single particle tracking and single molecule energy transfer. Wiley-VCH, Weinheim; 2009. https://doi.org/10.1002/9783527628360

29. Förster T. Zwischenmolekulare Energiewanderung Und Fluoreszenz. Ann Phys. 1948;6(2):55–75.

30. Behnam MAM, Nitsche C, Vechi M, et al. C-terminal residue optimization and fragment merging: discovery of a potent peptide-hybrid inhibitor of dengue protease. ACS Med Chem Lett. 2014;5:1037–42. https://doi.org/10.1021/ml500245v

31. Maus H, Barthels F, Hammerschmidt SJ, Kopp K, Millies B, Gellert A, et al. SAR of novel benzothiazoles targeting an allosteric pocket of DENV and ZIKV NS2B/NS3 proteases. Bioorg Med Chem. 2021;47(May):116392. https://doi.org/10.1016/j.bmc.2021.116392

32. Kalinin S, Peulen T, Sindbert S, Rothwell PJ, Berger S, Restle T, et al. A toolkit and benchmark study for FRET-restrained high-precision structural modeling. Nat Methods. 2012;9(12):1218–25. https://doi.org/10.1038/nmeth.2222

33. GmbH, A. T. ATTO 643 https://www.atto-tec.com/ATTO-643.html?language=en

34. Tarzia A. andrewtarzia/mol-ellipsize: v1.0.1 (v1.0.1). Zenodo. 2021. https://doi.org/10.5281/zenodo.5136958

35. Cheminformatics, O.-S. RDKit http://www.rdkit.org.

36. Henschel. Center of mass https://pymolwiki.org/index.php/Center_of_mass

37. Millies B, Von Hammerstein F, Gellert A, et al. Proline-based allosteric inhibitors of Zika and dengue virus NS2B/NS3 proteases. J Med Chem. 2019;62(24):11359–82. https://doi.org/10.1021/acs.jmedchem.9b01697

38. Weiss S. Fluorescence spectroscopy of single biomolecules. Science. 1999;283(5408):1676–83. https://doi.org/10.1126/science.283.5408.1676

39. Eggeling C, Fries JR, Brand L, Günther R, Seidel CAM. Monitoring conformational dynamics of a single molecule by selective fluorescence spectroscopy. Proc Natl Acad Sci U S A. 1998; 95(4):1556–61. https://doi.org/10.1073/pnas.95.4.1556

40. Widengren J, Kudryavtsev V, Antonik M, Berger S, Gerken M, Seidel CAM. Single-molecule detection and identification of multiple species by multiparameter fluorescence detection. Anal Chem. 2006;78(6):2039–50. https://doi.org/10.1021/ac0522759

41. Kühnemuth R, Seidel CAM. Principles of single molecule multiparameter fluorescence spectroscopy. Single Mol. 2001;2(4):251–4. https://doi.org/10.1002/1438-5171(200112)2:4<251::AID-SIMO251>3.0.CO;2-T

42. Deniz AA, Dahan M, Grunwell JR, Ha T, Faulhaber AE, Chemla DS, et al. Single-pair fluorescence resonance energy transfer on freely diffusing molecules: observation of Förster distance dependence and subpopulations. Proc Natl Acad Sci U S A. 1999;96(7):3670–5. https://doi.org/10.1073/pnas.96.7.3670

43. Margittai M, Widengren J, Schweinberger E, Schröder GF, Felekyan S, Haustein E, et al. Single-molecule fluorescence resonance energy transfer reveals a dynamic equilibrium between closed and open conformations of Syntaxin 1. Proc Natl Acad Sci U S A. 2003;100(26):15516–21. https://doi.org/10.1073/pnas.2331232100

44. Torres T, Levitus M. Measuring conformational dynamics: a new FCS-FRET approach. J Phys Chem B. 2007;111(25):7392–400. https://doi.org/10.1021/jp070659s

45. Chou TC, Talalay P. Quantitative analysis of dose-effect relationships: the combined effects of multiple drugs or enzyme inhibitors. Adv Enzyme Regul. 1984;22:27–55. https://doi.org/10.1016/0065-2571(84)90007-4

SUPPORTING INFORMATION

Additional supporting information can be found online in the Supporting Information section at the end of this article.